

The significance of the order of impregnation on the activity of vanadia promoted palladium-alumina catalysts for propane total oxidation

Tomas Garcia,^a Weihao Weng,^b Benjamin Solsona,^c Emma Carter,^d
Albert F. Carley,^d Christopher J. Kiely^b and Stuart H. Taylor*^d

Received 28th October 2010, Accepted 10th August 2011

DOI: 10.1039/c0cy00032a

The increased activity of alumina-supported palladium catalysts promoted with vanadium oxide has been investigated. Three different vanadium promoted Pd/Al₂O₃ catalysts with the same composition but synthesized employing sequential and co-impregnation were tested for the total oxidation of propane. The order of impregnation was critical to produce high activity catalysts. Vanadium and palladium co-impregnation on the Al₂O₃ support led to the most active catalyst, whereas the step-wise impregnated catalysts show a catalytic performance similar to or slightly better than unpromoted palladium catalysts. The high activity of the co-impregnated catalysts is related to the particle size and oxidation state of the palladium particles; and to the redox properties of vanadium species. The most active catalyst presents relatively large palladium particles in combination with increased reducibility of vanadium species and a relatively high amount of V⁴⁺ within the bulk of the catalyst and on the surface. STEM shows that, compared to catalysts containing only Pd or V, co-addition of the Pd and V species drastically altered the particle size distribution and morphology of the PdO_x particles, and simultaneously caused the monolayer dispersion of the VO_x species to become much patchier in nature. It also showed that the microstructure of the catalysts was similar for the different orders of impregnation, but some differences between the morphology of PdO_x particles were observed.

1. Introduction

Environmental legislation has imposed increasingly stringent targets for permitted levels of atmospheric emissions. In Europe the Gothenburg Protocol sets maximum permitted levels of emissions (emission ceilings) for each national signatory for four pollutants: sulphur, oxides of nitrogen, volatile organic compounds and ammonia. These ceilings, which must be met by 2010, were negotiated on the basis of scientific assessments of pollution effects and abatement options. Once the Protocol is fully implemented, Europe's sulphur emissions should be cut by at least 63%, its NO_x emissions by 41%, its ammonia emissions by 17% and its emission of volatile organic compounds (VOCs) by 40% compared to levels in 1990.¹ Similar reductions of levels of emission are also targets for legislation around the world.

The design and selection of new catalytic systems for the complete oxidation of hydrocarbons is an important task in environmental catalysis. Noble metal catalysts, in particular those based on palladium and platinum, have been widely studied for the combustion of alkanes due to their high reactivity.² Although noble metal catalysts have been studied by many groups, there is no consensus about the nature of the active species. Factors such as whether short chain alkane combustion is structure-sensitive^{3,4} or structure-insensitive^{5,6} and the oxidation state of the metal,^{7–9} are still under discussion.

The modification of noble metal supported catalysts, such as Au, Pd or Pt on Al₂O₃, TiO₂, ZrO₂ or CeO₂, by the addition of vanadium has received particular attention in recent years.^{10–18} In general, it has been observed that vanadium promoted catalysts present higher conversions, better selectivity and extended resistance to deactivation compared with unpromoted catalysts. Although there is no general agreement in the literature, alloying phenomena, modification of the support properties,¹¹ modification of the palladium particle size¹⁴ and modification of the redox properties^{9,10,13,15,16} of the catalysts are considered as the key factors to explain the improvement in catalytic performance when vanadium is incorporated.

^a Instituto de Carboquímica (CSIC), C/Miguel Luesma 4, 50018 Zaragoza, Spain

^b Department of Materials Science and Engineering, Lehigh University, 5 East Packer Avenue, Bethlehem, PA 18015-3195, USA

^c Departament d'Enginyeria Química, Universitat de València, C/Dr Moliner 50, 46100 Burjassot, Valencia, Spain

^d Cardiff Catalysis Institute, School of Chemistry, Cardiff University, Main Building, Park Place, Cardiff, CF10 3AT, UK.
E-mail: taylorsh@cardiff.ac.uk

Although the promotional effect of vanadium on palladium catalysts used for short chain alkane total oxidation has been established, there are no studies concerning the influence of the order of impregnation of the components on the activity for this reaction. However, for the reduction of NO in the presence of carbon monoxide, a strong influence of the preparation method of V-Pd catalysts has been reported,²¹ depending on which component is deposited first. Since most of the palladium catalysts synthesised to date for the combustion of lower alkanes have been prepared by impregnation, we have synthesised our supported Pd-V catalysts by varying the impregnation order: (i) deposition of vanadium on Pd/Al₂O₃, (ii) deposition of palladium on V/Al₂O₃ and (iii) co-impregnation of vanadium and palladium on the alumina support. A multi-technique characterisation approach has been adopted to study the catalysts, and elucidate the importance of catalyst preparation method in determining activity.

2. Experimental

2.1 Catalyst preparation

Co-impregnated catalysts were prepared by dissolving PdCl₂ (0.169 g, Aldrich 99%) in deionised water. The solution was heated to 80 °C and stirred continuously. An appropriate mass of ammonium metavanadate (2.80 g, Aldrich 99+) and oxalic acid (1.59 g, Aldrich 99+) were added to the solution. The required amount of alumina (Sasol, S_{BET} = 179 m² g⁻¹) was added to the heated solution and stirred at 80 °C to form a paste. The resulting paste was dried at 110 °C for 16 h. The catalyst contained a nominal concentration of 0.5 wt% Pd, and 6.0 wt% V.

A similar method was used to impregnate Al₂O₃ with vanadium (6.0 wt% V/Al₂O₃) and with palladium (0.5 wt% Pd/Al₂O₃). These materials were used as supports for the two step-impregnated catalysts: palladium was impregnated on the 6.0%V/Al₂O₃ catalyst and vanadium was impregnated on the 0.5%Pd/Al₂O₃ catalyst. The catalysts were then calcined in static air at 550 °C for 6 h. The range of catalysts prepared with their notation and a summary of the impregnation order are summarised in Table 1.

2.2 Catalyst characterisation

Catalyst surface areas were determined by multi point N₂ adsorption at 77 K, and data subjected to BET analysis. The CO uptake of the palladium catalyst was measured by pulse-adsorption of CO at 35 °C using an argon flow of 20 ml min⁻¹

and pulses of 0.2 ml of 10% CO in argon. Prior to CO uptake determination, all samples were treated under flowing hydrogen (50 ml min⁻¹) at 400 °C and then flushed with Ar at 400 °C (20 ml min⁻¹) for 60 min.

Temperature-programmed reduction (TPR) was carried out in a Micromeritics Autochem 2910 equipped with a TCD detector. The reducing gas used in all experiments was 10% H₂ in Ar, with a flow rate of 50 ml min⁻¹. The temperature range used was 295 °C–650 °C, and the heating rate was maintained at 10 °C min⁻¹ for all samples. Sample mass was 0.1 g for each experiment.

XPS measurements were made on a Kratos Axis Ultra DLD spectrometer at Kratos Analytical, Manchester UK, using monochromatised AlK α radiation, and analyser pass energies of 160 eV (survey scans) or 40 eV (detailed scans). Binding energies are referenced to the C(1s) peak from adventitious carbonaceous contamination, assumed to have a binding energy of 284.7 eV.

Electron Paramagnetic Resonance measurements were performed using ca. 5 mg of catalyst, which was placed into a high purity quartz EPR cell. The cw-EPR spectra were recorded on an X-band Bruker EMX spectrometer operating at 100 kHz field modulation, 10 mW microwave power and equipped with a high sensitivity cavity (ER 4119HS). All EPR spectra were recorded at 25 °C under air. EPR simulations were performed using the Sim32 software tool.²² Quantitative EPR measurements were carried out using a CuSO₄ standard.

Samples were prepared for scanning transmission electron microscopy (STEM) examination by grinding the powders between clean glass slides and then dispersing them onto a lacey carbon film supported on a Cu mesh grid. The samples were examined in an aberration corrected JEOL 2200FS (S)TEM operating at 200 kV, which was equipped with a Thermo Noran X-ray energy dispersive (XEDS) spectrometer.

2.3 Catalyst activity determination

Catalyst activity was determined using a fixed bed laboratory micro reactor. The reaction feed consisted of 5000 vppm hydrocarbon in air, a total flow rate of 50 ml min⁻¹ was used and catalysts were packed to a constant volume to give a gas hourly space velocity of 45 000 h⁻¹. Analysis was performed by on-line gas chromatography, using thermal conductivity and flame ionisation detectors. Catalytic activity was measured over the temperature range 100–550 °C and temperatures were measured by a thermocouple placed in the catalyst bed. Conversion data were calculated from the difference between

Table 1 Data for metal loadings, surface area and CO adsorption for the different Pd-V catalysts, and a summary of catalyst activity expressed as the temperature required to achieve 10, 50 and 90% propane conversion

Catalyst notation ^a	Impregnation order	Pd/%	V/%	S _{BET} /m ² g ⁻¹	CO _{uptake} /Pd/mol ratio	Temperature ^b /°C		
						T ₁₀	T ₅₀	T ₉₀
Al ₂ O ₃	None	—	—	179	—	—	—	—
Pd/A ^a	Pd only	0.5	0.0	165	0.21	325	380	450
V/A ^a	V only	0.0	6.0	170	—	395	> 500	> 500
(Pd + V)/A ^a	Co-impregnation of Pd and V	0.5	6.0	151	0.06	260	330	385
(Pd/A ^a) + V	Pd followed by V	0.5	6.0	152	0.10	325	385	460
(V/A ^a) + Pd	V followed by Pd	0.5	6.0	150	0.13	260	375	460

^a A = Al₂O₃. ^b Expressed as the temperature required for 10, 50 and 90% propane conversion.

inlet and outlet concentrations. Catalytic conversion data were reproducible within a few % and all carbon balances were $100 \pm 10\%$.

3. Results and discussion

Table 1 shows a summary of the range of catalysts used in this study and their BET surface areas. As expected, there was a reduction of the catalyst surface area as palladium and/or vanadium was impregnated onto the alumina support. The palladium loading of the samples was relatively low. No difference in the surface area was observed between Pd/V catalysts prepared by the different methods, even though the co-impregnated catalyst was calcined once and the other two catalysts were calcined twice. It is generally accepted that vanadia is very well dispersed by alumina and that the maximum capacity of this support to retain molecularly dispersed vanadium corresponds to 3.6–4.9 VO_x units per nm^2 .^{19,20} From these values, the percentage of a theoretical vanadia monolayer on the samples was estimated and corresponds approximately to *ca.* 80% of the complete monolayer.

Fig. 1 shows the variation of propane conversion with reaction temperature for the mixed Pd/V catalysts. For comparative purposes, the catalytic activity of 0.5 wt%Pd/ Al_2O_3 and 6 wt%V/ Al_2O_3 are also reported. CO_2 was the main reaction product for all the catalysts, although in the case of the V/A catalyst propylene was also observed, albeit in minor amounts at low conversion. The V/A catalyst without palladium showed the lowest activity, and the V/Pd catalyst prepared by co-impregnation was the most active catalyst at all temperatures. Table 1 summarises the temperatures observed for *ca.* 10%, *ca.* 50% and *ca.* 90% conversion. There is a clear promotional effect of vanadium on catalyst activity in the case of (V + Pd)/A and (V/A) + Pd catalysts at low reaction temperatures. Only the catalyst prepared by co-impregnation was more active than the unpromoted palladium catalyst over the whole temperature range, and this shows the importance of the preparation method in the final performance of the Pd/V/ Al_2O_3 catalysts.

TPR is often a useful technique for understanding the activity of oxidation catalysts and hydrogen is commonly used to provide model data on the reduction behaviour of the catalyst. Fig. 2 shows the hydrogen TPR profiles for the V/ Al_2O_3 and Pd-V/ Al_2O_3 catalysts. The Pd-free vanadium

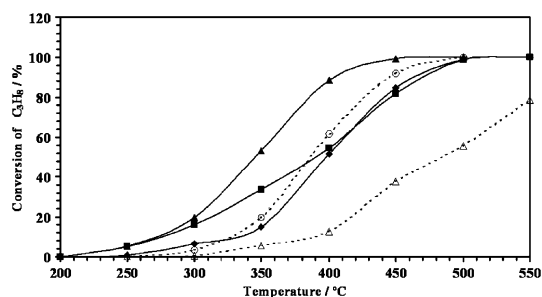


Fig. 1 Comparison of catalytic activities of several metal oxide catalysts: \blacktriangle (Pd + V)A; \blacksquare (V/A) + Pd; \blacklozenge (Pd/A) + V; \circ Pd/A; \triangle V/A. Conditions: GHSV = $45\,000\text{ h}^{-1}$, 0.5% propane and 20% O_2 in He.

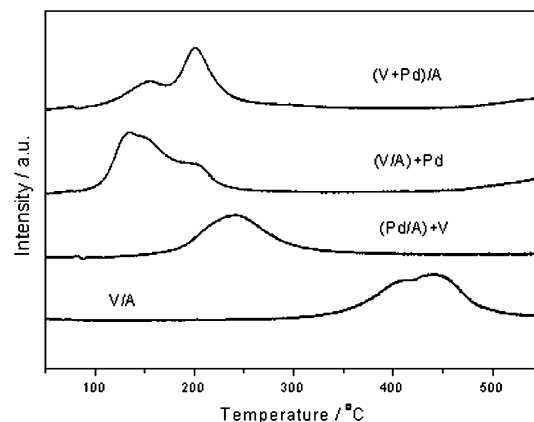


Fig. 2 Temperature programmed reduction profiles for the Pd/V/ Al_2O_3 catalysts. Conditions: $20\text{ }^\circ\text{C min}^{-1}$, 50 ml min^{-1} , 10% H_2 in Ar.

catalyst (V/A) shows a broad feature centred at $440\text{ }^\circ\text{C}$ with a shoulder at $410\text{ }^\circ\text{C}$, indicating the existence of two kinds of vanadium species. A shift to lower temperatures of the reduction features was observed for all of the mixed Pd/V catalysts, showing that the presence of palladium increases the reducibility of the vanadium species. Several groups have previously observed that the addition of palladium strongly promoted the reduction of vanadium oxide at lower temperatures on alumina supported catalysts.^{10,15,21} It is likely that the increased ease of vanadium reduction due to the addition of palladium operates by a spillover mechanism,^{13,15} as hydrogen dissociatively chemisorbs at the palladium surface and the resulting atomic hydrogen species effect the reduction of the vanadium. The reduction of vanadium may proceed *via* the formation of a vanadium bronze, and it has been demonstrated that such a phase can be formed on alumina supported catalysts at temperatures as low as $100\text{ }^\circ\text{C}$.²³ Both the shift to lower reduction temperatures and the peak distribution depend on the preparation method (Fig. 2). A single very broad feature centred at $240\text{ }^\circ\text{C}$ is present in the case of Pd/ Al_2O_3 impregnated with vanadium, whereas the 6 wt%V/ Al_2O_3 catalyst impregnated with palladium exhibits two main peaks around $135\text{ }^\circ\text{C}$ and $205\text{ }^\circ\text{C}$, the former comprising of two components. These peaks could be attributed to the existence of vanadium species in a different intimate contact with palladium particles, which could affect their reducibility. The presence of vanadium species with different degrees of aggregation/coordination as in the unpromoted sample can not be ruled out. Finally, the TPR profile of the catalyst prepared by co-impregnation also presents two main reduction peaks at $150\text{ }^\circ\text{C}$ and $200\text{ }^\circ\text{C}$, with the higher temperature reduction peak more intense. To summarise, the first hydrogen reduction peak for the (V/A) + Pd catalyst appears at $135\text{ }^\circ\text{C}$, at $150\text{ }^\circ\text{C}$ in the case of (V + Pd)/A and at $240\text{ }^\circ\text{C}$ for (Pd/A) + V. Hence there does not appear to be any direct correlation between the ease of reducibility and oxidation activity of the catalysts, although those catalysts showing a vanadium promoting effect at low temperature also show a hydrogen reduction feature at low temperature.

Unfortunately, no clear conclusions could be obtained about the direct reduction of the palladium species, as the experimental system only allowed reduction to be performed

at temperatures above ambient. No peaks could be detected in the TPR profiles which could clearly be assigned to PdO reduction, as this would proceed at room temperature under flowing hydrogen during the stabilisation period prior to the analysis.

In order to probe surface palladium sites CO chemisorption was used and the results are summarised in Table 1. The CO uptake is represented by CO/Pd, which is the molar ratio of adsorbed CO to total palladium in the catalyst. It is worth pointing out that CO uptake cannot be ascribed to CO adsorption on vanadium sites in the bi-component catalysts, since the V/Al₂O₃ catalyst did not show any CO uptake. The impregnation of 0.5 wt%Pd/Al₂O₃ with 6 wt% vanadium ((Pd/A) + V) decreased the CO uptake from 0.21 to 0.10. This suggests that the impregnated vanadium is either partially covering the palladium particles, or its addition resulted in larger palladium particles and reduced dispersion. Impregnating palladium onto V/Al₂O₃ produced the greatest number of CO chemisorption sites among the bimetallic catalysts and hence the greatest palladium dispersion. However, it should be noted that the number of palladium sites did not vary greatly with the order of impregnation, and the addition of vanadium, regardless of the order of impregnation, decreased the number of palladium sites.

The values presented in Table 1 clearly show that the fraction of exposed palladium atoms presents initially on Pd/A were decreased in the presence of vanadium. According to Neyertz,²⁴ this behaviour is due to the fact that the palladium crystals in the (V/A) + Pd sample are located on the vanadium monolayer and these are larger than those supported on the bare alumina, hence the presence of a monolayer of VO_x species on the alumina does not favour enhanced palladium dispersion. The authors claimed there was no evidence for vanadium migration onto the palladium surface. These conclusions also agree with results from Macleod and Lambert.²⁵

XPS studies have been carried out to further elucidate the influence of the presence of vanadium, and order of impregnation, on palladium dispersion, and to try to support conclusions from the CO uptake results outlined above. It is possible that decreased CO uptake on the incorporation of vanadium could be due to a decrease of palladium dispersion or partial covering of the palladium particles by vanadium species. Thus, the binding energy and the relative surface concentrations of Pd/V in various Pd catalysts are given in Table 2. Different Pd/V relative surface concentrations were detected depending on the preparation method. Whilst the co-impregnated catalyst shows a Pd/V atom ratio close to the theoretical value, this ratio was increased in the case of (V/A) + Pd, which is in agreement with the increase in CO uptake results shown in Table 1 and previously published data.^{24,25} The Pd/V atom ratio for the (Pd/A) + V sample calculated from the XP spectra (Table 2) is lower than the co-impregnated catalyst value. This fact could be due to VO_x species decorating the Pd/A. However, the decrease is less than would be expected if the VO_x were a continuous film on top of the Pd/A, which again is in agreement with the CO uptake results. Finally, the palladium and vanadium co-impregnated catalyst showed similar theoretical and experimental Pd/V atom ratios together with the lowest CO uptake. It is difficult to draw any

definitive detailed conclusions on the palladium and vanadium dispersion from the XPS data as the relative surface concentrations could be changing due to a number and combination of reasons. It could be that dispersion of either or both components is changing, morphology of the components is altered by the preparation method or one component is preferentially depositing on the surface of the other. For the reasons outlined above a detailed STEM study was undertaken to probe more fully the structure and dispersion of the palladium and vanadium components and the results of this study are presented later.

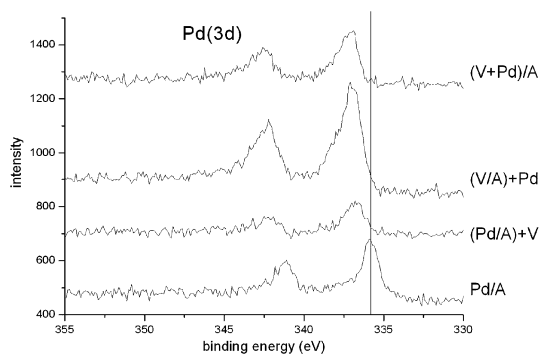
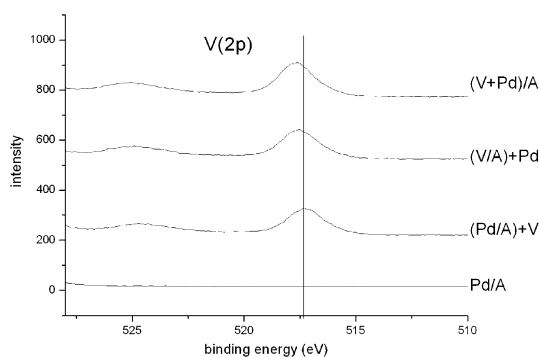
In addition, XPS results (Table 2 and Fig. 3) show the Pd(3d_{5/2}) binding energy values and spectra for the differently prepared catalysts. There is a clear chemical shift for all of the vanadium-containing catalysts compared with the pure Pd/A material. The Pd(3d_{5/2}) peak appears at 335.6 eV, indicating a metallic state.²⁶ On the other hand the vanadium promoted Pd/Al₂O₃ samples presents a mean binding energy value of ca. 337.1 eV corresponding to palladium oxide, PdO.^{27–29} According to this, it has been recently reported²⁴ that the formation of new electrophilic sites by the presence of VO_x species in a vanadium promoted Pd/Al₂O₃ catalyst is responsible for the existence of Pd species in an Pd⁺² oxidation state. Therefore, we can conclude that the origin of the observed binding energy shift (Fig. 3) is due to the presence of metallic palladium in Pd/A and PdO in the other catalysts.

Smaller shifts are observed in the corresponding V(2p_{3/2}) binding energies (Table 2, Fig. 4), which correspond to V⁵⁺ for the V/A catalyst. The V(2p_{3/2}) peaks from all the V-containing samples exhibit an asymmetry to the low binding energy side, indicating the presence of reduced vanadium species, most probably V⁴⁺. We have curve-fitted the peaks to 2 components (an example is shown in Fig. 5) and the resulting V⁴⁺ contents are shown in Table 2. The V⁵⁺–V⁴⁺ binding energy difference was found to be in the range 1.2–1.5 eV, confirming the identity of the V⁴⁺ species. The O(1s) binding energy was checked for all the catalysts, and in all cases a single peak centred at 531.2 eV was observed. This was not surprising as oxygen is the predominant element on the surface of the catalysts, and subtle modification of oxygen species associated with the palladium and vanadium components would be swamped by signals from the catalyst support.

Following on from the XPS studies, EPR spectroscopy was also used to examine the influence of the support and the palladium on the electronic properties of the paramagnetic vanadyl ions. The room temperature X-band EPR spectra for V and Pd/V catalysts are shown in Fig. 6. As expected no EPR signal was observed from the diamagnetic 0.5 wt% Pd/Al₂O₃ catalyst. The EPR spectra are typical of a vanadyl anisotropic powder spectrum, exhibiting primarily axial symmetry. Hyperfine coupling due to the interaction of the vanadium nuclear spin [$I(v) = 7/2$] with the unpaired d¹ electron leads to eight observable hyperfine lines in both the parallel and perpendicular direction. The linewidth of each resonance is broad due to a combination of spin–spin broadening and the completely random orientation of the species with respect to the external magnetic field. The spin Hamiltonian parameters were extracted by computer simulations. Good agreement was found between the *g* values (*i.e.*, $g_x = 1.975$, $g_y = 1.975$, $g_z = 1.94$) and A

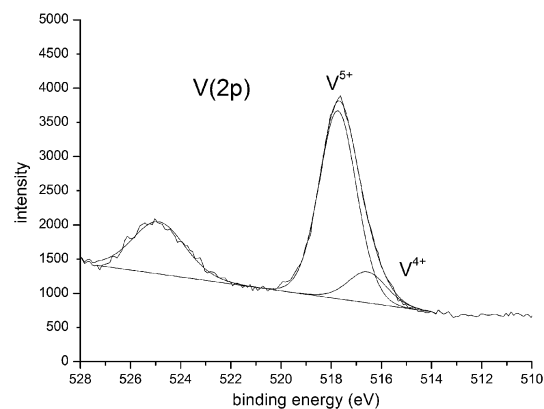
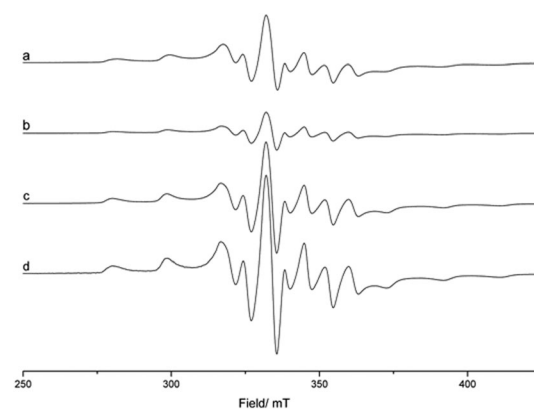
Table 2 Summary of EPR and XPS results

EPR			XPS				
Catalyst	Number of spins g^{-1}	% V species present as V^{4+}	Pd($3d_{5/2}$) binding energy (eV)	V($2p_{3/2}$) binding energy (eV)	Pd/V molar (expt)	Pd/V molar (theory)	% V species present as V^{4+}
Pd/A	—	—	335.6	—	—	—	—
V/A	5.29×10^{19}	7.5	—	517.8	—	—	5.3
(Pd + V)/A	9.39×10^{19}	13.2	337.0	517.7	0.044	0.040	10.3
(Pd/A) + V	5.56×10^{19}	7.8	336.9	517.3	0.029	0.040	6.2
(V/A) + Pd	9.76×10^{19}	13.7	337.2	517.6	0.098	0.040	14.4

**Fig. 3** Pd(3d) X-ray photoelectron spectra for the four Pd-containing catalysts.**Fig. 4** V(2p) X-ray photoelectron spectra for the four Pd-containing catalysts.

values (*i.e.*, $A_x \sim 180$ MHz, $A_y \sim 160$ MHz, $A_z \sim 500$ MHz) for each sample and these parameters are entirely consistent with an assignment based on a distorted octahedral environment for V^{4+} . The similarities in the g and A values implies that the amount of tetragonal distortion (and hence local environment) is similar in all the catalysts.

A quantitative EPR study of the catalysts was also undertaken and the amount of paramagnetic V^{4+} species was found to depend on the presence of palladium and the preparation method (Table 2). We observe (Tables 1 and 2) that the two best catalysts (Pd + V)/A and (V/A) + Pd contain approximately twice the concentration of V^{4+} (13–14%) compared to the more poorly performing (Pd/A) + V and V/A samples (7–8%). The quantitative data for the different vanadium species from EPR are in excellent agreement with the XPS derived values, and any differences are probably due to the

**Fig. 5** Example curve-fit of a V(2p) spectrum used to determine the V^{4+} content of the catalysts; the spectrum shown is for the (V/A) + Pd catalyst.**Fig. 6** cw-EPR X-band spectra [25 °C] of (a) 6 wt% V/ Al_2O_3 , (b) 6 wt% V on Pd/ Al_2O_3 , (c) 0.5 wt% Pd on V/ Al_2O_3 and (d) V/ Pd (co-impregnation) on Al_2O_3 .

fact that EPR is a bulk technique and XPS is surface specific. The increased concentration of V^{4+} species from XPS and EPR is consistent with the TPR data, indicating that the presence of palladium modifies the redox characteristics of the vanadium.

Detailed bright field (BF) and high angle dark field (HAADF) STEM imaging experiments, coupled with XEDS analyses, have also been performed on this systematic series of catalysts. Fig. 7(a) and (b) are a complementary pair of low magnification BF- and HAADF-STEM images from the

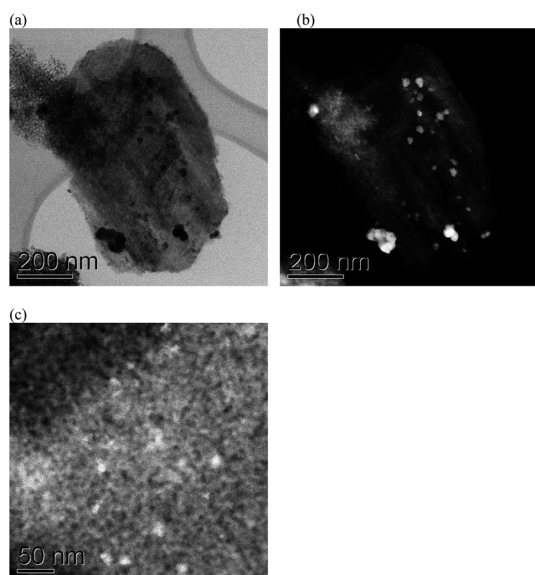


Fig. 7 A complementary pair of (a) BF-STEM and (b) HAADF-STEM images from the Pd/Al₂O₃ catalyst showing irregularly shaped 20–100 nm PdO_x particles. (c) A higher magnification HAADF image showing the additional presence of numerous 5–10 nm Pd-containing clusters.

monometallic Pd/Al₂O₃ catalyst showing irregularly shaped 20–100 nm palladium particles. Higher magnification HAADF images (Fig. 7(c)) show the additional presence of numerous 5–10 nm Pd-containing clusters scattered over the porous Al₂O₃ support. By way of contrast, no bulk V-containing species at all could be detected in BF or HAADF-STEM images from the V/Al₂O₃ catalyst (Fig. 8(a) and (b)) suggesting that the VO_x species are highly dispersed over the support. This supposition is confirmed by the XEDS spectrum presented in Fig. 8(c), which was acquired from an extended area of the Al₂O₃ support, in which a small V K peak at 4.948 keV can be seen in addition to the stronger Al K peak at 1.486 keV. This V K peak could be detected anywhere on the support, suggesting that the vanadium is homogeneously distributed over the Al₂O₃ support particles.

The morphology of the co-impregnated (Pd + V)/A catalyst is quite different from either of its single constituent counterparts as shown in Fig. 9(a) and (b). The majority of the PdO_x particles adopted a much more well defined oblong morphology, and lie in the 10–50 nm size range. In addition, the population of 5–10 nm palladium-containing clusters that was previously observed in the Pd-only sample was completely absent, this material presumably having been subsumed into the larger oblong PdO_x particles. BF and HAADF-STEM images of the oblong particles (Fig. 9(c) and (d)) also showed them to have quite rough pock marked surfaces and possibly some internal porosity. Some STEM-XEDS analysis of the (Pd + V)/A catalyst has also been attempted as shown in Fig. 10. XEDS spectra obtained from the oblong particles (Fig. 10(a), (b)–region 1) and Fig. 10(c)) show a strong Pd signal as expected. Interestingly in the HAADF image (Fig. 10(b)) the Al₂O₃ support appears dark in some places (*e.g.* region 2) but bright in others (region 3). The corresponding XEDS spectra (Fig. 10(d) and (e) respectively) show the absence of V in

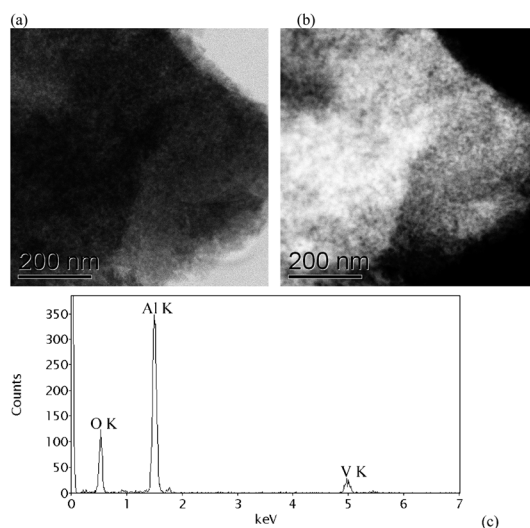


Fig. 8 A complementary pair of (a) BF-STEM and (b) HAADF-STEM images of the V/Al₂O₃ catalyst in which no bulk-V containing species are detectable. The XEDS spectrum acquired from an extended area of the support (c) shows the presence of a V K peak at 4.948 keV in addition to the Al K peak at 1.486 keV confirming that the V is highly dispersed on the support.

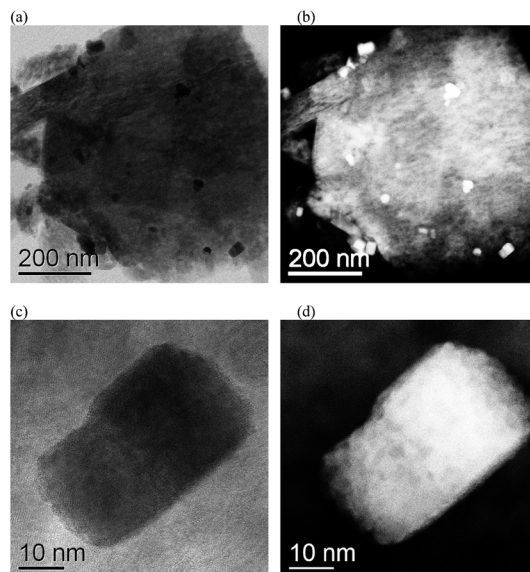


Fig. 9 A complementary pair of (a) BF-STEM and (b) HAADF-STEM images from the co-impregnated Pd + V/Al₂O₃ catalyst showing characteristic rectangular shaped 10–50 nm PdO_x particles. Higher magnification BF- and HAADF-STEM views of an isolated oblong PdO_x particle are shown in (c) and (d) respectively.

the darker regions, and its definite presence in the brighter regions. Hence this implies that the bright and dark contrast of the Al₂O₃ support in the HAADF image (Fig. 10(b)) is in fact atomic number (*Z*) contrast arising from the presence or absence of the VO_x overlayer. Interestingly the VO_x material often seems to be depleted in the vicinity of large oblong PdO_x particles, but is still present in areas where there are relatively few or no PdO_x particles. Hence we have clearly demonstrated that co-addition of the Pd and V species drastically alters the

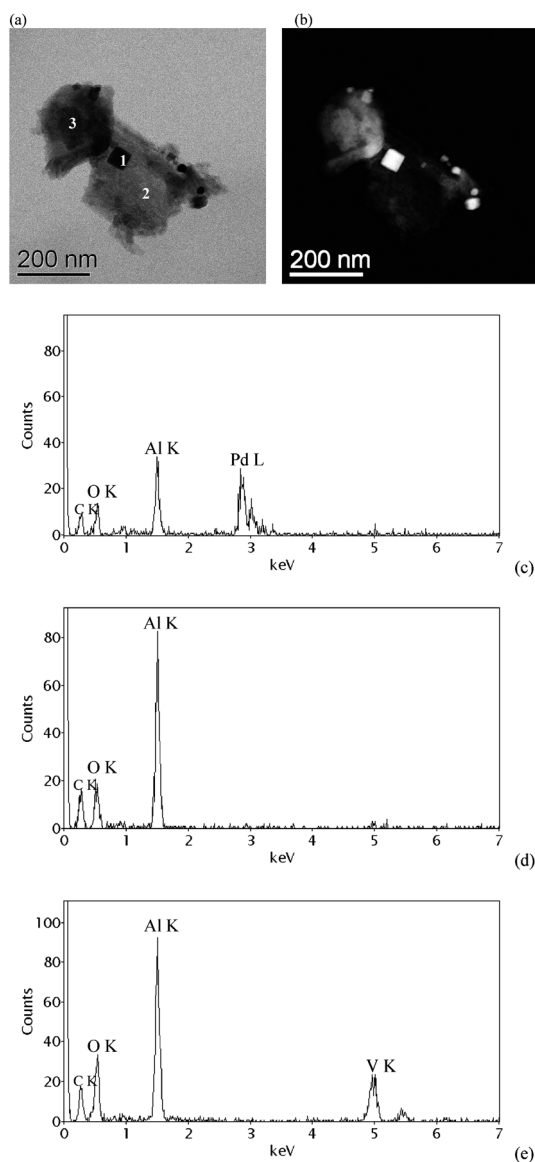


Fig. 10 A complementary pair of (a) BF-STEM and (b) HAADF-STEM images from the co-impregnated Pd + V/Al₂O₃ catalyst. The XEDS spectra shown in (c), (d) and (e) were acquired from the regions labelled 1, 2 and 3 respectively in (a).

particle size distribution and morphology of the PdO_x species, and this is consistent with a decrease of the palladium dispersion that was postulated from CO chemisorption and XPS studies. STEM also indicates that there was little or no decoration of the palladium particles by VO_x species. The coexistence of palladium and vanadium also simultaneously causes the initial monolayer dispersion of the VO_x species to become much more patchy in nature.

Fig. 11 shows representative HAADF-STEM images from the sequentially impregnated (V/A) + Pd and (Pd/A) + V catalyst materials. In each case, the microstructure found is more reminiscent of the co-impregnated (Pd + V)/A catalyst, as opposed to the Pd/Al₂O₃ or V/Al₂O₃ materials. The (V/A) + Pd sample (Fig. 11(a) and (b)) exhibits fairly irregular shaped PdO_x particles. The (Pd/A) + V sample (Fig. 11(c) and (d)) shows PdO_x particles that have a slightly more well developed

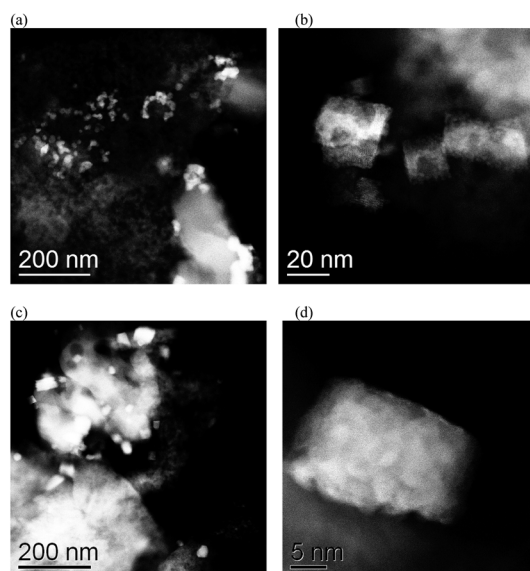


Fig. 11 Representative HAADF-STEM images from the sequentially impregnated (a and b) (V/A) + Pd catalyst, and (c and d) (Pd/A) + V catalyst.

oblong morphology than those for (V/A) + Pd, but they are still not quite as distinctive as those seen in the co-impregnated Pd-V/Al₂O₃ catalyst. Both of the sequentially deposited variants (*i.e.* (V/A) + Pd and (Pd/A) + V) are devoid of the sub-10 nm Pd containing clusters found in the Pd/Al₂O₃ sample.

In order to try to explain the general catalytic behaviour of the mixed Pd/V catalysts, several different factors need to be taken into account. These are the role of the palladium sites, the role of the vanadium sites and the role of the interface formed between palladium, vanadium and alumina. Regarding the role of the palladium sites, supported Pd or PdO catalysts have been extensively used for the total oxidation of VOCs.^{30,31} Nevertheless, their behaviour is not well understood, and for example, the nature of the true active phase (metal or metal oxide)^{32,33} and the role of the palladium particle size remain a matter of debate. Whilst several authors have not observed any correlation between particle size and turnover frequency,³⁴ others have observed a strong dependence of activity on particle size for alkane oxidation over Pd/Al₂O₃ catalysts.³ Moreover, in the case of Pd/V/Al₂O₃ catalysts, Ferreira *et al.*¹⁵ established that benzene oxidation is a structure sensitive reaction. Similar conclusions were reported by Dancheva *et al.*³⁵ These authors claimed that the vanadium promoting effect was related to the activation of oxygen on the metal particles, which enables the reverse oxidation of V⁴⁺, and this leads to an equilibrium in the redox process. These authors proposed a redox mechanism to explain the process: (i) oxidation of V⁴⁺ to V⁵⁺ and Pd⁰ to Pd²⁺ by the oxygen; (ii) reduction of V⁵⁺ to V⁴⁺ by the hydrocarbon. In this mechanism V³⁺ was very stable. We can reach a similar conclusion concerning the propane catalytic combustion results on Pd/V/Al₂O₃ catalysts presented here, as the (Pd + V)/A catalyst with the lowest CO uptake value, showed the highest catalytic activity. Therefore, propane combustion on this type of catalyst also seems to be a structure sensitive reaction, although no direct relationship can be found between CO

uptake values and catalytic activity, although it should be noted that palladium dispersion did not vary greatly between catalysts impregnated with palladium and vanadium, and this was confirmed by STEM. There were subtle differences between the morphology of the PdO_x nanoparticles depending on the order of vanadium and palladium impregnation and these could also influence the catalytic activity.

According to the mechanism above, the role of the V-species on activity must also be considered, since it is the key factor responsible for the vanadium promoting effect at low temperature. According to the EPR results, a clear correlation was identified between the V⁴⁺ content and catalytic activity, in the temperature range 250–350 °C (Table 2 and Fig. 1), the two best catalysts (Pd + V)/A and (V/A) + Pd contained approximately twice the concentration of V⁴⁺ as compared to the poorly performing (Pd/A) + V and V/A catalysts. Thus, the higher amount of V⁴⁺ present in V/Pd-catalysts suggests that the above redox mechanism could be operating, and the incorporation of Pd into V/Al₂O₃ catalysts leads to a dramatic increase in the reducibility of vanadium, which is more evident in the best performing, (Pd + V)/A and (V/A) + Pd catalysts.

It is worth mentioning that at higher temperatures the correlation above stated between the amount of V⁴⁺ and the catalytic activity breaks down. This can possibly be a consequence of the increasingly more predominant role of mass transport limitations on the reaction rate and to a diminishing role of vanadium sites for propane adsorption, with a possible increasing role of palladium sites for adsorption and catalytic reaction. Therefore, the role of the interface formed between palladium, vanadium and alumina are of crucial importance in the final performance of the vanadium promoted Pd/Al₂O₃ catalysts. The catalyst preparation method is affecting the final characteristics of the palladium and vanadium sites, and hence it has an important role in determining activity. It is worth highlighting that for environmental applications, total conversion of volatile organic compounds is the major aim, so that co-impregnation is the more suitable preparation method for this application.

4. Conclusions

The total oxidation of propane on alumina supported Pd/V catalysts is strongly dependent on the order of impregnation used for preparation. In particular, the co-impregnated catalyst is more active than the materials impregnated sequentially, since an adlayer structure has been obtained. The superior performance has been related to the presence of large palladium particles in combination with other factors. It has been established that propane total oxidation over the Pd/V catalyst is not solely a palladium size dependant reaction, and modification of the redox properties is also a determining factor for the activation of propane. Varying the preparation method of V/Pd catalysts leads to different reducibility of vanadium species (as seen by TPR) and different proportions of V⁴⁺/V⁵⁺ in both the surface and bulk of the catalysts (as determined by XPS and EPR). The most active catalysts, (Pd + V)/A and (V/A) + Pd, contain the highest surface concentrations of V⁴⁺ species. However, in the catalyst (V + Pd)/A the reduced V species are in close proximity to Pd²⁺ but not under

the palladium particles and this gives rise to the best catalyst performance. STEM shows that, compared to catalysts containing only Pd or V, co-addition of the Pd and V species drastically altered the particle size distribution and morphology of the PdO_x species, and simultaneously caused the monolayer dispersion of the VO_x species to become much patchier in nature. It also showed that the microstructure of the catalysts was similar for the different orders of impregnation, but some differences between the morphology of PdO_x particles were observed.

Acknowledgements

We would like to thank the EPSRC, EC, and Cardiff University for financial support. We are also grateful to Dr Damien Murphy for helpful discussions.

References

- Commission of the European Communities, Brussels, COM (2002) 44 final, 2002/0035 (CNS).
- T. V. Choudhary, S. Banerjee and V. R. Choudhary, *Appl. Catal., A*, 2002, **234**, 1.
- R. F. Hicks, H. Qi, M. L. Young and R. G. Lee, *J. Catal.*, 1990, **122**, 280.
- C. A. Mueller, M. Maciejewski, R. A. Koeppl and A. Baiker, *Catal. Today*, 1999, **47**, 245.
- T. R. Baldwin and R. Burch, *Appl. Catal.*, 1990, **66**, 337.
- F. H. Ribeiro, M. Chow and R. A. Dalla Betta, *J. Catal.*, 1994, **146**, 537.
- R. Burch and F. J. Urbano, *Appl. Catal., A*, 1995, **124**, 121.
- J. N. Carstens, S. C. Su and A. T. Bell, *J. Catal.*, 1998, **176**, 136.
- A. Ishikawa, S. Komai, A. Satsuma, T. Hattori and Y. Murakami, *Appl. Catal., A*, 1994, **110**, 61.
- T. Garcia, B. Solsona, D. M. Murphy, K. L. Antcliff and S. H. Taylor, *J. Catal.*, 2005, **229**, 1.
- C. Neyertz, M. Volpe and C. Gigola, *Appl. Catal., A*, 2004, **277**, 137.
- L. S. Escandón, S. Ordóñez, F. V. Diez and H. Sastre, *Catal. Today*, 2003, **78**, 191.
- S. Dancheva, L. Ilieva, N. Kotsev and A. Andreev, *Collect. Czech. Chem. Commun.*, 1994, **59**, 1922.
- M. Vassileva, E. Moroz, S. Dancheva, V. Ushakov and A. Andreev, *Appl. Catal., A*, 1994, **112**, 141.
- R. S. G. Ferreira, P. G. P. de Oliveira and F. B. Noronha, *Appl. Catal., B*, 2004, **50**, 243.
- D. Andreeva, T. Tabakova, L. Ilieva, A. Naydenov, D. Mehanjiev and M. V. Abrashev, *Appl. Catal., A*, 2001, **209**, 291.
- D. Andreeva, R. Nedyalkova, L. Ilieva and M. V. Abrashev, *Appl. Catal., A*, 2003, **246**, 29.
- M. Vassileva, A. Andreev and S. Dancheva, *Appl. Catal.*, 1991, **69**, 221.
- G. Deo and I. Wachs, *J. Catal.*, 1994, **146**, 323.
- J. Le Bars, A. Auroux, M. Forissier and J. C. Vedrine, *J. Catal.*, 1996, **162**, 250.
- C. Neyertz and M. Volpe, *Colloids Surf., A*, 1998, **136**, 63.
- T. Spalek, P. Pietrzyk and Z. Sojka, *J. Chem. Inf. Model.*, 2005, **45**, 18.
- E. van der Heide, M. Zwinkels, A. Gemitsen and J. Sholten, *Appl. Catal., A*, 1999, **86**, 181.
- C. Neyertz, M. Volpe, D. Perez, I. Costilla, M. Sanchez and C. Gigola, *Appl. Catal., A*, 2009, **368**, 146.
- N. Macleod and R. M. Lambert, *Catal. Lett.*, 2003, **90**, 111.
- K. Otto, L. P. Haack and J. E. deVries, *Appl. Catal., B*, 1992, **1**, 1–12.
- K. S. Kim, A. F. Gossmann and N. Winograd, *Anal. Chem.*, 1974, **46**, 197.
- Y. Bi and G. Lu, *Appl. Catal., B*, 2003, **41**, 279.
- E. H. Voogt, A. J. M. Mens, O. L. J. Gijzeman and J. W. Geus, *Surf. Sci.*, 1996, **350**, 21.

-
- 30 E. van der Heide, M. Zwinkels, A. Gemitsen and J. Sholten, *Appl. Catal., A*, 1999, **86**, 181.
- 31 P. Papaefthimiou, T. Ioannides and X. E. Verykios, *Appl. Catal., B*, 1997, **13**, 175.
- 32 R. Burch and F. J. Urbano, *Appl. Catal., A*, 1995, **124**, 121.
- 33 R. F. Hicks, H. Qi, M. L. Young and R. G. Lee, *J. Catal.*, 1990, **122**, 295.
- 34 R. J. Farrauto, J. K. Lampert, M. C. Hobson and E. M. Waterman, *Appl. Catal., B*, 1995, **6**, 263.
- 35 M. Vassileva, A. Andreev, S. Dancheva and N. Kotsev, *Appl. Catal.*, 1989, **49**, 125.